POLARIMETRIC SAR TOMOGRAPHY

Stéphane Guillaso and Andreas Reigber

Technical University Berlin, Computer Vision and Remote Sensing
Franklinstr. 28/29, Sekr. FR3-1, 10587 Berlin, Germany
stephane AT cs.tu-berlin DOT de, anderl AT cs.tu-berlin DOT de

ABSTRACT

In this paper, different approaches of airborne SAR tomography are presented. A SAR tomographic data acquisition system can be represented like an antenna array. The use of high-resolution methods is indicated to the concept of aperture synthesis for 3D-imaging using SAR data. Techniques presented are the standard FOURIER-, CAPON-based beamforming methods to improve the resolution quality. In order to estimate the nature of retrieved target, a polarimetric approach is introduced based on the modified high-resolution MUSIC algorithm. Finally, experimental results are shown using a multibaseline data set acquired in L-band by DLR's experimental SAR (E-SAR) on a test site near Oberpfaffenhofen / Germany.

1 INTRODUCTION

SAR tomography is the extension of conventional two-dimensional SAR imaging principle to three dimensions [1],[2]. A real three-dimensional imaging of a scene is achieved by the formation of an additional synthetic aperture in elevation by a coherent combination of images acquired from several parallel flight tracks. The introduction of tomographic SAR offers the possibility of a direct localisation of all scattering contributions in a volume, which normally appear superimposed in a conventional two-dimensional image. This greatly extends the potential of SAR, particularly for the analysis of volume structures, like for example forests or urban areas.

This paper presents different investigations on high-resolution approaches, like CAPON [2], [3], MUSIC, in order to improve the resolution achieved using the standard beamforming FOURIER-based method. These methods are often employed for so-called DoA (direction of arrival) estimation of received waves, using an antenna array. Basically, a multibaseline acquisition system represents an antenna array and these methods can be applied in order to determine the height of dominant scatterers. This is presented in section 2.

A logical extension of the tomographic data processing consists in using the vectorial properties of electromagnetic waves. In section 3, an introduction to the estimation of the polarisation state of retrieved target, in order to determinate its nature, is proposed. This approach is based on a modified signal model adapted to MUSIC algorithm, taking into account the vectorial nature of the backscattered wave. In section 4, the efficiency of

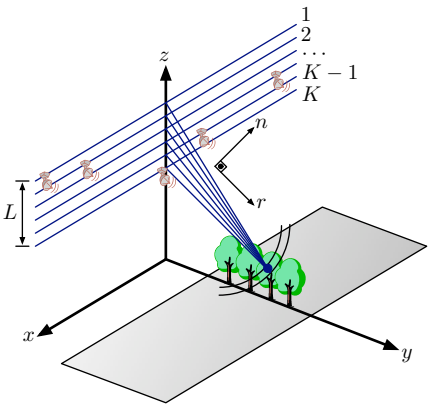

Fig. 1: Principle of multibaseline SAR tomography. An area is seen from K sensors on parallel flight tracks.

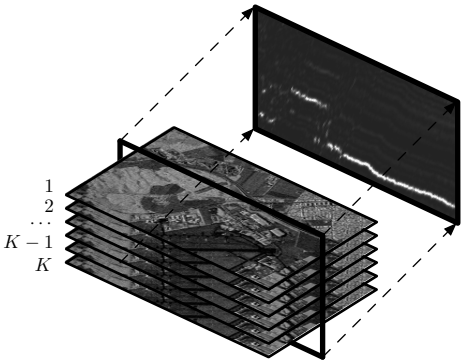

Fig. 2: Extraction of 3D profile from K SAR images.

this polarimetric interferometric SAR data analysis is demonstrated, using 14 fully polarimetric SAR images, obtained from DLR-ESAR airborne sensor in L-band repeat-pass mode.

2 MONOCHANNEL SAR TOMOGRAPHY

SAR tomography consists in focusing several SAR images in the third dimension, in order to image volumetric area, such as forests or cities. This means to form a synthetic aperture along the direction perpendicular to azimuth and to the line of sight. This principle is illustrated by Fig. 1. The geometry of a tomographic data acquisition uses typically K interferometric tracks non uniformly spaced, which observe the same scene. From this K images, 3D profiles might be extracted make it possible to detect target under a covered volume or to generate 3D images of building.

Tomographic SAR data can be processed using the SPECAN (SPECtral ANalysis) algorithm. This is a two step algorithm, based on a deramping of the signal, followed by a subsequent focusing step. The deramping step corrects the quadratic phase variation, occurring during tomographic data acquisition [1]. Its principle is to multiply the received signal by a deramping function, which accounts for the geometry of the data acquisition. After deramping, the spatial frequency f_z of the signals depend only on the height of the occurring scattering processes. In Fig. 3, it is demonstrated that a target with a positive height z has a constant positive spatial frequency f_z, while a target with a height below the reference height is characterised by a constant negative spatial frequency. Thus, after deramping, the height of a scatterer can be revealed by a spectral estimation method: Measuring the power of frequencies components in the deramped signal is means measuring the power of the backscattering in a certain height.

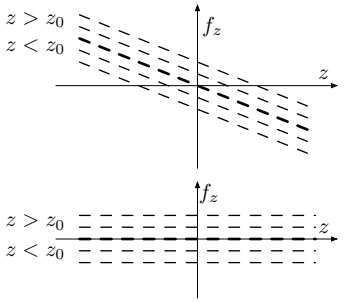

Fig. 3: Deramping of the tomographic signal in the time-frequency (z-f_z) plane.

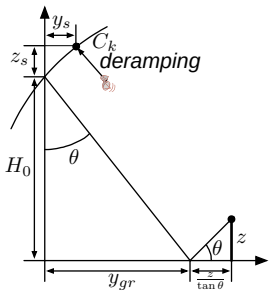

Fig. 4: Geometric parameters used during tomographic data processing.

The focusing step is performed using standard high resolution methods such as Fourier, Capon, and MUSIC. A tomographic data acquisition system can be compared to an antenna array, which is used to localise different sources of radiation. In the case of SAR tomography, this antenna array is spanned by the parallel tracks, i.e. in the direction perpendicular to azimuth and line-of-sight. Classically, the system is constituted by K sensors, or interferometric paths. The signal x_k received by each sensor k provided by D scatterers localised at height $\{z_d\}_{d=1}^{D}$ may be written as:

$$x_k = \sum_{d=1}^{D} \mathrm{e}^{i\phi_k(z_d)} \cdot s_d + n_k \quad \text{with} \quad \phi_k(z_d) = -\frac{4\pi}{\lambda} d_k(z_d) = -\frac{4\pi}{\lambda} \sqrt{(H_0 - z_d + z_s)^2 + (y_{gr} + y_s + \frac{z_d}{\tan\theta})^2} \tag{1}$$

where each term of the Eq. 1 is defined by Fig. 4 and n_k represents a circular Gaussian white noise. Using a vectorial notation Eq. 1 may be written as:

$$\vec{x} = [x_1 \cdots x_K]^T = [A]\vec{s} + \vec{n} \quad \text{with} \quad [A] = [\vec{a}(z_1) \cdots \vec{a}(z_D)] \quad \text{and} \quad \vec{a}(z_d) = [\mathrm{e}^{i\phi_1(z_d)} \cdots \mathrm{e}^{i\phi_K(z_d)}]^T \tag{2}$$

The $[A]$ matrix, with dimension $K \times D$, contains the phase response due to the sensor geometry only and each vector $\vec{a}(z_d)$ represents the steering vector corresponding to the d-th scatterer. All high resolution methods are based on a covariance matrix formulation defined as:

$$[R] = \langle \vec{x}\vec{x}^{\dagger} \rangle \quad \text{which is estimated by} \quad [\hat{R}] = \sum_{n=1}^{N} \vec{x}_n \vec{x}_n^{\dagger} \tag{3}$$

where N represents the number of samples used to generate the covariance matrix $[\hat{R}]$. The condition: $N > K$ is necessary in order to obtain a non-singular matrix $[\hat{R}]$.

To focus tomographic SAR data, two approaches based on high-resolution methods are existing: classical and subspace-based. Classical methods are standard beamforming / spectral estimation methods; famous representatives are the FOURIER and the CAPON approach. The main idea is to focus the system on a certain height, corresponding to the height of a scatterer. To do that, the range of valid heights is scanned in order to find maximum of power. The estimated powers given by FOURIER-, $\hat{P}_F(z)$, and CAPON-, $\hat{P}_C(z)$, based beamforming approaches are function of the height z:

$$\hat{P}_F(z) = \frac{\vec{a}(z)^{\dagger}[\hat{R}]\vec{a}(z)}{K^2} \quad \text{and} \quad \hat{P}_C(z) = \frac{1}{\vec{a}(z)^{\dagger}[\hat{R}]^{-1}\vec{a}(z)} \tag{4}$$

where $\vec{a}(z)$ represents the steering vector given by Eq. 2. It must be mentioned that the CAPON estimator corresponds to a minimisation of the received power in all direction except those of the observed scatterer.

The second category is based on the principle of subspace estimation. It gives an estimation of the scatterer height with an infinite resolution, independently of the signal-to-noise ratio. The most known subspace methods are MUSIC, ESPRIT and WSF [4]. These methods are based on a eigendecomposition of the observed covariance matrix, $[\hat{R}] = [\hat{E}][\hat{\Lambda}][\hat{E}]^{\dagger}$, where $[\hat{E}]$ represents the matrix of eigenvectors of $[\hat{R}]$, and $[\Lambda]$ is a diagonal matrix formed with the eigenvalues of $[\hat{R}]$. Classically, the eigenvector space is decomposed into two subspace called signal, $[\hat{E}_S]$, and noise, $[E_N]$, with $[E] = [E_S|E_N]$. The MUSIC method exploits the orthogonal property between steering vectors and the noise subspace $[E_N]$. The pseudo-beamforming of MUSIC, $\hat{P}_M(z)$, is given by:

$$\hat{P}_M(z) = \frac{1}{\vec{a}^{\dagger}([\hat{E}_N][\hat{E}_N]^{\dagger})\vec{a}} \tag{5}$$

The term pseudo-beamforming is employed here because in the ideal case, each time that z corresponds to a z_d, the scalar product is zero and $\hat{P}_M(z = z_d)$ becomes ∞. This means that the value of the power is using only to find the target height.

3 INTRODUCTION TO POLARIMETRIC SAR TOMOGRAPHY

The use of the vectorial properties of electromagnetic waves is a logical extension to the tomographic data processing. An extension of the MUSIC algorithm [5], allows to retrieve the polarisation information associate to dominant scatterers. This approach is based on the use of JONES-vector formulation.

The polarisation state of an electromagnetic wave is defined by its JONES-vector, $\vec{E}$, which contains complete information about amplitudes and phases of electromagnetic field components. The JONES-vector can be written using two polarisation angles: γ and δ, and the polarisation ratio $\rho_{\vec{E}}$:

$$\vec{E} \overset{\text{def}}{=} E \begin{bmatrix} \cos\gamma \\ \sin\gamma \mathrm{e}^{i\delta} \end{bmatrix} = E\cos\gamma \begin{bmatrix} 1 \\ \rho_{\vec{E}} \end{bmatrix} \quad \text{with} \quad \rho_{\vec{E}} = \tan\gamma \mathrm{e}^{i\delta} \tag{6}$$

Using a similar form than Eq. 2, let $\vec{y}$, $\vec{s}$, and $\vec{n}$ denote the received signal, the source amplitude vector, and the noise vector, respectively. Then, $\vec{y}$ has the following form:

$$\vec{y} = [A] \cdot \vec{s} + \vec{n} \tag{7}$$

where the $2K \times D$ matrix $[A]$ is the steering matrix with columns $\vec{a}_d$ as the steering vectors:

$$\vec{a}_d = [\vec{E}_d^T \cdot \mathrm{e}^{i\phi_1(z_d)} \quad \cdots \quad \vec{E}_d^T \cdot \mathrm{e}^{i\phi_K(z_d)}]^T \quad \text{with} \quad \vec{E}_d = [\cos\gamma_d \quad \sin\gamma_d \mathrm{e}^{i\delta_d}]^T, \qquad d = 1, 2, \cdots, D \tag{8}$$

$\phi_k(z_d)$ is given by Eq. 1.

In [5], a polarisation estimation method using the noise subspace eigenvectors of $[\hat{R}]$, is described. It can be shown that each steering vector $\vec{a}_d$ may be written as the linear combination of two direction vectors $\vec{b}_1(z_d)$ and $\vec{b}_2(z_d)$, which are associated to the scattering height z_d and two arbitrary orthogonal polarisations. The steering vector $\vec{a}_d$ can be written as:

$$\vec{a}_d = [B_d] \cdot \vec{f}_d \quad \text{with} \quad [B_d] = [\vec{b}_1(z_d) \quad \vec{b}_2(z_d)], \qquad d = 1, 2, \cdots, D \tag{9}$$

where $\vec{f}_d$ represents a 2×1 vector consisting of the linear combination coefficient.
In order to simplify the calculation process, $\vec{b}_1(z_d)$ and $\vec{b}_2(z_d)$ are normalised:

$$\vec{b}_1'(z_d) = \frac{\vec{b}_1(z_d)}{\|\vec{b}_1(z_d)\|} \quad \text{and} \quad \vec{b}_2'(z_d) = \frac{\vec{b}_2(z_d)}{\|\vec{b}_2(z_d)\|}, \qquad d = 1, 2, \cdots, D \tag{10}$$

Let define $\vec{a}_d'$ as the normalised steering vector of $\vec{a}_d$:

$$\vec{a}_d' = \frac{\vec{a}_d}{\|\vec{a}_d\|} = [B_d']\vec{f}_d' \quad \text{with} \quad [B_d'] = [\vec{b}_1'(z_d) \quad \vec{b}_2'(z_d)], \qquad d = 1, 2, \cdots, D \tag{11}$$

It can be shown that the ratio between the two elements of $\vec{f}_d'$ corresponds to the polarisation ratio $\rho_{\vec{E}}$. The estimation of $\vec{f}_d'$ is given by calculating the eigenvector of the Hermitian matrix $[B_d']^\dagger [E_N][E_N]^\dagger [B_d']$, corresponding to the smallest eigenvalue.
Finally, the two polarimetric angles γ_d and δ_d can be determined uniquely from:

$$\begin{aligned} \gamma_d &= \tan^{-1}\left(\left|\tfrac{1}{\rho_{\vec{E}_d}}\right|\right) \\ \delta_d &= -\arg \rho_{\vec{E}_d} \end{aligned} \quad , \qquad d = 1, 2, \cdots, D \tag{12}$$

4 EXPERIMENTAL RESULTS

The different methods presented above have been applied to a L-band data set of the E-SAR. The data were acquired in May 1998 on the test site of Oberpfaffenhofen/Germany. During the campaign fully polarimetric data sets were recorded from K =14 parallel flight tracks with a respective distance of approximatively 20 meters. The airplane used by the E-SAR is equipped with a high-precision positioning system, which allows an absolute estimation of the antenna tracks with an accuracy of few centimetres. With this data the errors arising from the aircraft movements are compensated by a new approach of motion compensation during SAR processing [6]. Additionally, a very precise velocity and range delay variation compensation have been carried out. To minimise small errors in the absolute positioning of the aircraft, also a calibration of the image phases, based on the response of a single corner reflectors is performed.

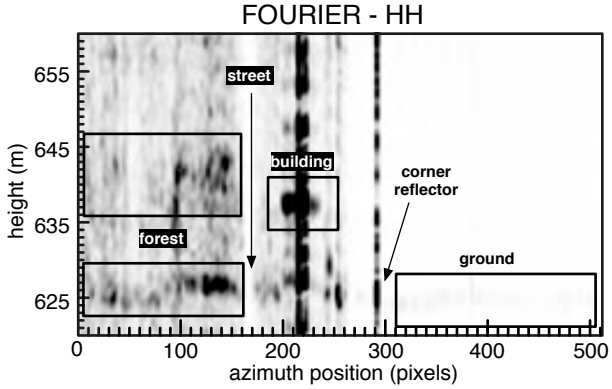

Fig. 5: FOURIER-based height/azimuth slice tomogram.

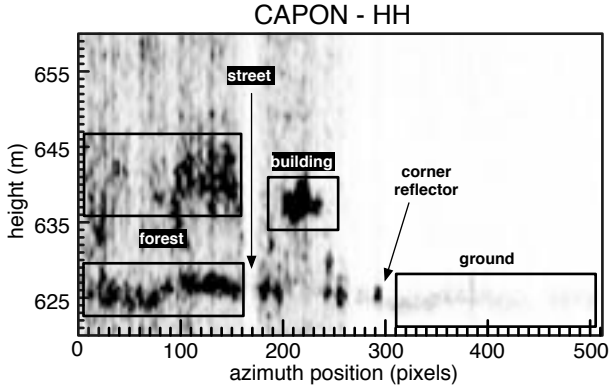

Fig. 6: CAPON-based height/azimuth slice tomogram.

Fig. 5 and 6 represent height/azimuth slices of tomograms obtained using FOURIER and CAPON approaches, respectively. The left part of the scene is constituted by a dense spruce forest with a height of 15 to 20 meters [1]. Then, the azimuth slice crosses a street, some bushes and a building. The right part of the scene consists of nearly flat grass land with a corner reflector. The CAPON-based approach makes it possible to reduce the sidelobes, particularly strong in case of the building and the corner reflector. The ground under the forest is better visible in Fig. 6, the same holds for the canopy density. It is also possible to determinate a height of about 20 meters for the trees .

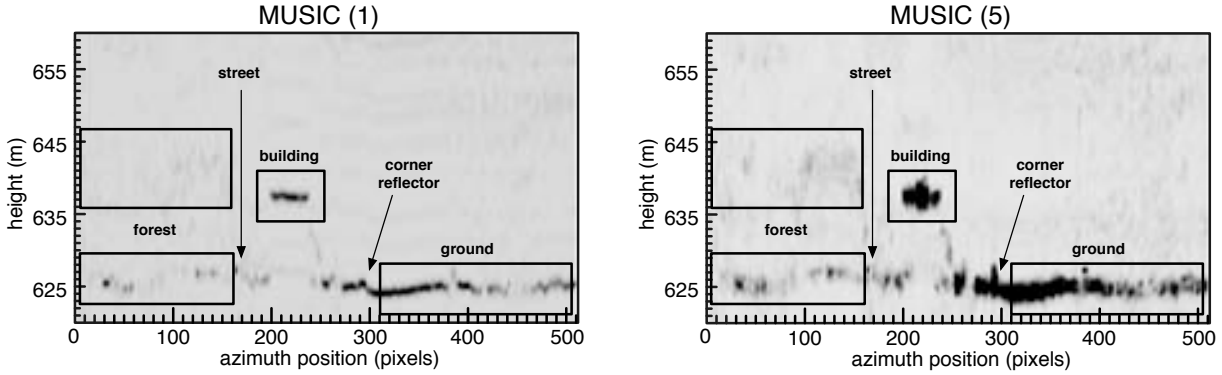

(a) One scatterer assumed

(b) Five scatterers assumed

Fig. 7: Polarimetric MUSIC-based height/azimuth slice tomogram.

Fig. 7(a) and 7(b) represent the same height/azimuth slices than Fig. 5 and 6 by using the polarimetric MUSIC approach with partial polarimetric data (HH and VH). In Fig. 7(a), only one scatterer was assumed, whereas in Fig. 7(b), 5 scatterers were considered in the processing. The shape of the building is better visualised, as well as the ground of the grass field in Fig. 7(a), when only one scatterer is assumed. It is also possible to estimate the height of the corner reflector. Over the forest, ground and canopy reflection can be expected. These results are better when using 5 scatterers (in Fig. 7(b)), but make no sense for the building and specially for the grass area.

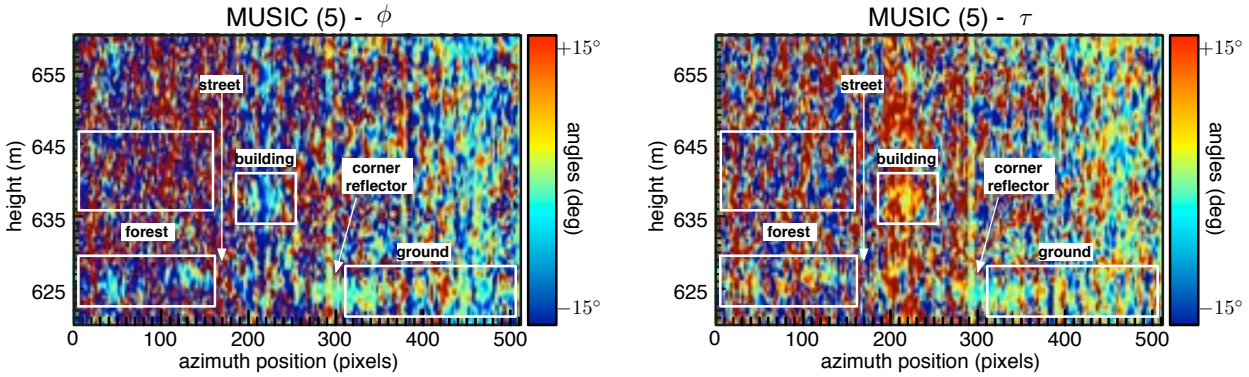

(a) Orientation angle ϕ

(b) Ellipticity angle τ

Fig. 8: Angles characterising the polarisation ellipse.

The two polarimetric angles γ and δ are estimated using the approach given in section 3. From the spheric angle, it is possible to estimate the orientation, ϕ, and ellipticity, τ, angles characterising the polarisation ellipse. The relations between all different angles are:

$$\tan(2\phi) = \tan(2\gamma) \cdot \cos\delta \quad \text{and} \quad \sin(2\tau) = \sin(2\gamma) \cdot \sin\delta \tag{13}$$

Fig. 8(a) and 8(b) represent the ϕ and τ angles retrieved using the polarimetric MUSIC approach, assuming 5 scatterers. These results show that the retrieved polarisations are media depending. The polarisation state responses of the forest ground and the grass field have not the same polarimetric response, but a similar one. Over the building, the polarimetric response is significantly different than over the other media. Over the forest canopy, polarimetric responses are random, as it can be expected from the random behaviour of this kind of media. Please note that in areas with no backscattering (air, underground, etc.), the signal consists only of noise. Here, principally no valid estimates can be derived.

This polarimetric approach of the SAR tomography shows the polarimetric behaviour depending with the media observed and makes it possible to characterise targets in terms of height position but also by their physical properties.

5 CONCLUSION

This paper presents a introduction in polarimetric SAR tomography. In a first part, high resolution methods were used to generate high quality tomograms. The different approaches proposed are FOURIER and CAPON-based methods, applied on monochannel SAR data. Results given by these approaches make it possible to retrieve the position of target, even in case of covered areas like forests. The use of CAPON reduce the sidelobe effect observed with FOURIER-beamforming. The height estimation of the different targets corresponds to the ground truth. In a second part, a polarisation state estimation of target using MUSIC approach was defined. This approach is based on a extension of the MUSIC algorithm taking into account the vectorial nature of electromagnetic waves. Results show a improvement of the target localisation but also describe the polarimetric behaviour over different media.

6 ACKNOLEDGEMENTS

This work was supported by the German Science Foundation DFG, under project No. RE 1698/1.

References

[1] A. Reigber and A. Moreira, "First demonstration of airborne sar tomography using multibaseline l-band data," *IEEE Transactions on Geoscience and Remote Sensing*, vol. 38, pp. 2142–2152, September 2000.

[2] F. Lombardini and A. Reigber, "Adaptive spectral estimation for multibaseline sar tomography with airborne l-band data," in *Proceedings of IGARSS'03*, (Toulouse, France), July 2003.

[3] J. Capon, "High resolution frequency wavenumber spectrum analysis," *Proceedings of the IEEE*, vol. 57, pp. 1408–1418, August 1969.

[4] P. Stoica and R. Moses, *Introduction to Spectral Analysis*. N. J.: Prentice Hall, 1997.

[5] E. Ferrara and T. Parks, "Direction finding with an array of antennas having diverse polarizations," *IEEE Transactions on Antennas and Propagation*, vol. AP-31, pp. 231–236, March 1983.

[6] P. Prats, A. Reigber, J. J. Mallorqui, and A. Broquetas, "Efficient detection and correction of residual motion errors in airborne sar interferometry," in *Proceedings of IGARSS'04*, pp. 992–995, September 2004.